Journal of The Electrochemical Society, **154** (11) B1132-B1137 (2007)
0013-4651/2007/154(11)/B1132/6/$20.00 © The Electrochemical Society

Preparation and Characterization of CO-Tolerant Pt and Pd Anodes Modified with SnO_2 Nanoparticles for PEFC

Tatsuya Takeguchi,[a,*,z] Yuri Anzai,[a] Ryuji Kikuchi,[b,*] Koichi Eguchi,[b,*] and Wataru Ueda[a]

[a]*Catalysis Research Center, Hokkaido University, Kita-ku, Sapporo 001-0021, Japan*
[b]*Department of Energy and Hydrocarbon Chemistry, Graduate School of Engineering, Kyoto University, Nishikyo-ku, Kyoto 615-8510, Japan*

The Pd/C and Pt/C anodes modified with SnO_2 nanoparticles for the polymer electrolyte fuel cell (PEFC) were investigated using pure and 500 ppm CO-contaminated H_2 as fuel gas. Modification of the Pd/C anode with SnO_2 nanoparticles enhanced the cell performance in pure H_2, while modification of the Pt/C anode a little lowered the performance. The effect of SnO_2 addition on the performances of the cell with the Pd anode in CO-contaminated H_2 was examined. The cell voltage with the $Pd/SnO_2/C$ anode in 500 ppm CO-contaminated H_2 was 0.41 V at a current density of 0.2 A/cm^2, while that in pure H_2 was 0.59 V. The $Pd/SnO_2/C$ anode exhibited good tolerance to CO poisoning, since the anode adsorbed CO more weakly. Neither electrochemical oxidation of CO nor shift reaction contributed to the CO tolerance of the $Pd/SnO_2/C$ anode.

Manuscript submitted November 13, 2006; revised manuscript received June 29, 2007.
Available electronically September 7, 2007.

Polymer electrolyte fuel cell (PEFC) is the system which can efficiently convert the chemical energy to electricity, since the efficiency of fuel cells is not restricted by Carnot's theorem. The system is an attractive power source as a clean power generator for domestic use or automobiles. Since PEFC can generate electricity on site, the transmission loss can be minimized. When PEFC is applied as domestic use, the high energy utilization is expected, because the waste heat can be utilized as air conditioners and hot water by cogeneration systems. However, there are a lot of tasks to be solved in PEFC systems; one of the most important tasks is to lengthen the life of the system. High reliability and durability are required to spread the domestic-use PEFC system. At present, the cell voltage at a constant same current density gradually decreases with operation time; therefore, it is being aimed for the declining rate to be less than 2.0 mV per 1000 h in the current density range from 0.1 to 0.3 A/cm^2. This target is expected to be achieved under the following conditions: the entrance temperature of the cell ranges from 70 to 80°C; the fuel utilization ranges from 70 to 80%; air utilization ranges from 30 to 60%. At the declining rate of 2.0 mV per 1000 h, the voltage declines by 70 mV for 40,000 h. It is corresponding to 10-year operation including 10 h operation a day.[1]

The natural gas is expected as one of the promising raw materials of fuel for the domestic use of PEFC, because the natural gas is provided as city gas. When natural gas is reformed with steam to produce H_2, a considerable amount of CO is also produced. When the reformed fuel gas is fed to the anode of PEFC, CO in the reformed fuel gas poisons the Pt anode. To decrease the CO concentration, the fuel processor of the PEFC system normally comprises a steam reformer, a shift converter, and a CO preferential oxidation unit. In this CO removal unit, the CO concentration can be reduced to less than 10 ppm from 10 or 20%, but this unit is very bulky. Cu-based catalysts[2] were ordinarily used as the shift-converter catalyst in plants; however, it is difficult to use the Cu-based catalyst in the domestic-use PEFC system. The PEFC system would be frequently turned on and off. When the system is turned off, Cu catalysts will be easily oxidized by steam and air, and eventually deactivated. Therefore, precious metal catalysts such as Pt catalysts supported on CeO_2-containing oxides were used in the PEFC system. On the other hand, Pd,[3] Au,[4] Pt or Ru[5] is used as the catalyst for preferential oxidation of CO at low temperature, and Pd/SnO_2,[3] Pt/SnO_2, and Ir[6] are expected to be used for preferential oxidation of CO. Among them the Ru catalyst exhibited the high performance for preferential oxidation of CO and the long-term stability under low O_2/CO molar ratio.[5] In any case, considerable amounts of precious metals were used in both a shift converter unit and a CO preferential oxidation unit, resulting in high cost. Moreover, this complicated system containing a CO-removal unit led to low efficiency and reliability. Therefore, it is earnestly desired to develop CO-tolerant anode catalysts.

Because of these backgrounds, excellent CO-tolerant catalysts like Pt–Ru alloy on carbon have been developed,[7] but Ru is also a precious material. Therefore, it is important to develop the CO-tolerant anode without Ru in order to cut the cost of the PEFC. There are several CO-tolerant Pt-containing anodes, such as Pt/Sn, Pt/W, Pt/Mo,[8] Pt/Ru/Sn, Pt/Ru/W, Pt/Ru/Mo,[9] Pt/MoO_3,[10] Pt–TaO_x, and Pt–NbO_x.[11] Even nonalloy-type anode catalysts showed the CO tolerance because the interaction between Pt and metal oxides affected the nature of Pt catalyst.[12] For instance, the performance of the cell with the Pt/MoO_x anode was almost comparable to the PtRu (1:1) in 100 ppm CO-contaminated H_2.[9] However, further improvement of the anode catalyst is required to spread the domestic-use PEFC systems, since higher CO tolerance reduces the size of the PEFC system and increase stability. Moreover, the compact direct-methanol PEFC system is being developed, because it does not need the heavy and bulky external fuel reformer. It is expected to be applied especially to power electric vehicles. In this system, various CO-tolerance PtM alloy anodes are also actively investigated.[13-15] An alloy of Pt and Sn is used as the anode catalyst for direct methanol[13] and direct ethanol fuel cells.[16]

The Pt/SnO_2 anode catalysts were proposed for direct ethanol fuel cells.[17-19] The electrochemical property of Pt/SnO_2 was investigated in detail.[20] The authors developed Pt/SnO_2 anode catalyst for PEFC using CO-contaminated H_2.[21,22] In this study, the CO-tolerant Pt and Pd anode catalysts modified with SnO_2 were investigated. Both of Pt and Pd anode catalysts have the functions of H_2 adsorption and dissociation. In expectation of the interaction between Pt or Pd and SnO_2, Pt and Pd anodes were modified with SnO_2. To make the active surface area larger and to increase the number of contact points between Pt or Pd and SnO_2, SnO_2 nanoparticles were prepared.[23] Since Pd/SnO_2 and Pt/SnO_2 were known to be active for the low-temperature oxidation of CO, CO poisoning of Pt-group metals is expected to be avoided.[6] The catalysts in this study were prepared by the impregnation method, and catalyst metals were dispersed on carbon black. The electrochemical activities of the catalysts were examined with a single cell in pure and 500 ppm CO-contaminated H_2 gas, since the higher CO tolerance the anode catalysts have, the more merit PEFC has.

---

[*] Electrochemical Society Active Member.
[z] E-mail: takeguch@cat.hokudai.ac.jp

Experimental

Preparation of electrode catalysts.— All catalysts used in this study were prepared by the impregnation method. First, the SnO_2 nanoparticles were prepared by the following sol-gel method from tin grains.[23] A 3 g portion of tin, shot, 99.999% (Wako Pure Chemical Industries, Ltd.) and 10 g of citric acid (Wako Pure Chemical Industries, Ltd.) were dissolved in the 300 mL of an 8 M nitric acid solution (Kanto Chemical Co., Inc.). An aqueous solution of NH_3 (Wako Pure Chemical Industries, Ltd.) was added to the mixed solution until the pH value reached 8. Next, this solution was refluxed at 100°C for 2 h. After cooling down, the solution was centrifuged and washed with distilled water and ethanol to collect the $Sn(OH)_4$ sol. The resulting sol containing ethanol and carbon black, Vulcan XC72R (Cabot Corp.) were mixed with desired amounts of the aqueous solutions of $Pd(NO_2)_2(NH_3)_2$ (Tanaka Kikinzoku Kogyo K.K.) containing 4.574 wt % Pd or $Pt(NO_2)_2(NH_3)_2$ (Tanaka Kikinzoku Kogyo K.K.) containing 4.552 wt % Pt. The mixed suspension of Pd or Pt and carbon black was prepared. Each mixture was kept on a steam bath at 80°C until the solution was evaporated to form powders. The dried powders were heated to 300°C in 70 mL/min flow of 100% N_2 at heating rate of 10°C/min, and the temperature was kept for 30 min. The weight ratio of Pd or Pt/SnO_2/carbon black was 1 / 1 / 4. Thus, Pd/SnO_2/C, Pt/SnO_2/C, Pd/C, and Pt/C catalysts were prepared. Reduction was carried out in the cell under the same operation condition at 70°C for the generation experiment.

Characterization of the anode catalysts.— The samples with and without reduction treatment were analyzed by X-ray diffraction (XRD). Morphology of the anode catalyst without reduction treatment was observed by Hitachi H-800 transmission electron microscope. A CHEMBET-3000 was used to evaluate the Brunauer-Emmett-Teller (BET) surface area of the anode catalyst without reduction treatment, based on the amount of N_2 adsorbed at the liquid nitrogen temperature. This apparatus was also used to determine the amount of CO adsorbed on precious metal. The ordinary CO pulse method was employed to investigate the catalyst temperature dependence of the amount of CO adsorbed. The amount of CO adsorbed was measured with reducing temperature. The weight of each sample was 50 mg. The flow rate of H_2/Ar and He was 70 mL/min. The volume of the one pulse was 0.288 mL.

The effect of the temperature on CO adsorption was investigated after the catalysts were reduced in 5% H_2/Ar at 100°C for 300 min. Then, He gas was fed, and the temperature was raised to 300°C. The CO pulse titration method was used to estimate the CO adsorption on the precious metal. To investigate the temperature dependence of CO adsorption, the following method was adopted. First, 50 mg of the sample was packed in the reactor, and He was fed to the sample. The sample was heated to 100°C at 10°C/min in 5% H_2/Ar and then kept at 100°C for 30 min. The sample was flushed with He for 5 min and was heated to 300°C at 10°C/min. The 0.288 mL portion of CO was pulsed every 2 min, until the intensity of the peak became constant. Another two 0.288 mL CO pulses were added for confirmation. Then the sample was cooled down to 270°C, and CO was pulsed in the same way. These procedures were repeated at 240°C, 210°C, 180°C, 150°C, 120°C, 90°C, 60°C and 25°C in the same way as mentioned above.

On the other hand, when the effect of the reduction temperature was investigated, the catalysts were reduced in 5% H_2/Ar at 100 or 200°C. Then, the catalysts were cooled to 25°C, and He was fed followed by CO pulse measurement.

X-ray photoelectron spectroscopy (XPS) was employed to determine the superficial composition of each catalyst with and without reduction treatment. These spectra were acquired on a JEOL JPS-9010MC using Mg Kα radiation at 10 kV and 10 mA. The base pressure was 6.0×10^{-9} Torr (8.0×10^{-7} Pa), while the operating pressure was around 5×10^{-7} Torr (6×10^{-5} Pa). The XP spectra were quantified by Gauss-Lorentz fitting to determine the area under the peaks.

Anodic voltammetry.— CO-stripping voltammetry experiments were carried out in 0.5 M H_2SO_4 with usual three-electrode arrangement in an electrochemical cell using Solartron 1287 electrochemical interface. A platinum rod with an outer diameter of 6.0 mm and Ag/AgCl (NaCl saturated) were used as counter and reference electrodes, respectively. The reference electrode has a potential of $E = +0.212$ V vs the reversible hydrogen electrode (RHE) and all potentials are referred to the RHE. The anode catalyst reduced at 100°C was loaded on the glassy carbon electrode, and it was used as a working electrode. After CO was supplied to the electrochemical cell for 1 h, bulk CO was removed by bubbling nitrogen through it for 15 min. The CO-stripping voltammograms were measured between −0.2 and 1.2 V (vs Ag/AgCl) with a scan rate of 20 mV/s.

Construction of membrane electrode assemblies (MEAs).— To prepare the electrode catalyst paste, *n*-butyl acetate (Wako Pure Chemical Industries, Ltd.), Nafion solution (Nafion perfluorinated ion-exchanged resin, 5 wt % solution in a mixture of lower aliphatic alcohols and water, Aldrich) and ion-exchanged water were mixed, and then the catalyst was added to the mixture in the ultrasonic wave bath. Finally, this mixture was put in the ultrasonic wave bath for 30 min. Next, to prepare the anode and cathode, the paste was painted with a spatula on a peace of carbon fiber paper (GDL P50T Paper, Ballard Material Products, Inc.) having an area of 5 cm^2 so that the loading of precious metal was 1 mg/cm^2. On the other hand, cathodes which have 2 mg/cm^2 of Pt were also made in the same way.

Electrolyte membrane (Nafion 117, perfluorinated membrane, 0.007 in. in thickness) was pretreated before use. The pretreatment process followed the conditions of standard membrane treatment which had been recommended by NEDO PEFC R&D project; the membrane was successively boiled in a 1 M H_2SO_4 aqueous solution for 1 h; in distilled water for 1 h; in a 1 M H_2O_2 aqueous solution for 1 h; and again in distilled water for 1 h. Thereafter, the surface of the pretreated electrolyte membrane was washed with ion-exchanged water. The membrane was sandwiched between the dried electrodes, and then the component was pressed at 2 MPa and 130°C for 10 min. The various anodes were prepared, whereas the cathodes of these membrane electrode assemblies (MEAs) were Pt/C in every case. These MEAs were kept under wet condition.

Measurement of cell performances (polarization properties).— After MEA was fastened with 3.5 N m, it was put in a single cell, FC05-01SP (Electro Chem, Inc.). Pure H_2 gas and a gaseous mixture of 22% O_2-78% N_2 were fed to the anode and the cathode at 100 and 200 mL/min, respectively. When the CO tolerances of the anode catalysts were examined, 500 ppm CO-contaminated H_2 was supplied. Both gases were humidified by bubbling in water at 73°C.

The polarization properties were measured on Autolab30-MF-SP by using General Purpose Electrochemical System for Windows version 4.9 (Autolab Eco Chemie B.V.). To avoid the loss of ionic conductivity by drying the electrolyte, MEAs were kept under the wet condition before putting in the single cell for measurement.

Results and Discussion

Cell performance.— The performances of the cells with various Pd and Pt anodes for electrochemical reactions were compared in Fig. 1. The cell with a Pt/C anode exhibited a higher performance than that with a Pd/C anode, as is expected from the fact that Pt has a higher activity for electrochemical oxidation of H_2 than Pd. The effect of SnO_2 addition to the Pt/C and Pd/C anodes was also examined. The terminal voltage of the cell with the Pt/C anode is 0.67 V at a current density of 0.2 A/cm^2, while that with the Pt/SnO_2/C anode is 0.64 V. This may be caused by the lower conductivity of SnO_2 than C or Pt. Moreover, the number of active sites may decrease, since the addition of SnO_2 partly blocks the active site of Pt particles.

On the other hand, the terminal voltage of the cell with the Pd/C anode is only 0.55 V at 0.2 A/cm^2. However, the voltage with a

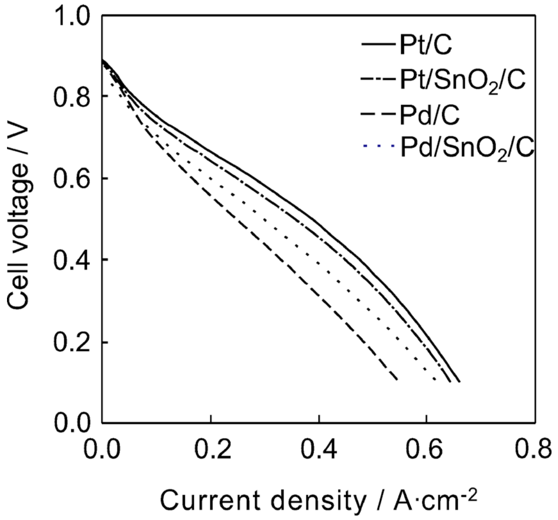

Figure 1. Comparison of the performances of PEFCs with various Pd and Pt anodes. Cathode: Pt/C; anode: Pt/C and Pd/C with/without SnO_2; anode gas: H_2; cathode gas: air; cell: 70°C, humidifier: 73°C.

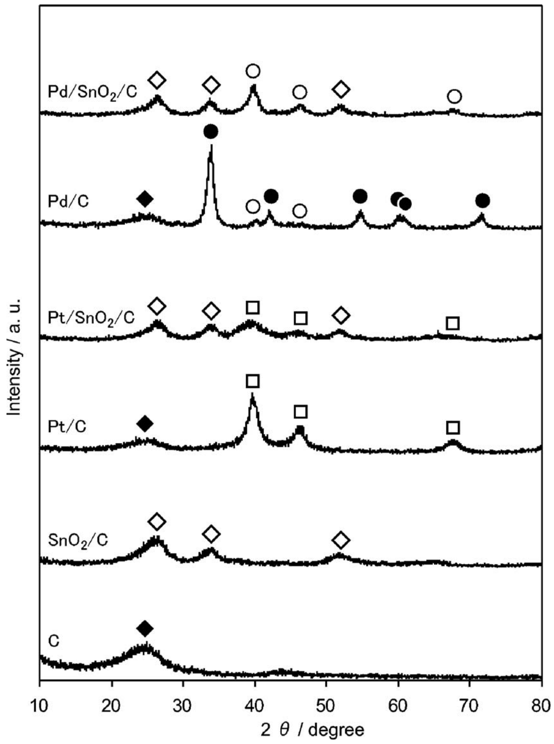

Figure 2. X-ray diffraction patterns of (SnO_2-modified) Pd and Pt anode catalysts. ○: Pd, ●: PdO, □: Pt, ◇ : SnO_2, ◆: C_3.

Pd/SnO_2/C anode rather increased to 0.59 V. Modification with SnO_2 clearly promoted the performance of a Pd/C anode, while the modification is deteriorating for the Pt/C anode. In general, the number of active sites is strongly related to the particle size of the catalyst metals. One of the possible reasons for these effects was that the SnO_2 addition may rather increase the dispersion of Pd particles, resulting in the increase in number of the precious metal active site for electrochemical H_2 oxidation at the catalyst surface. Otherwise, the modification with SnO_2 may change the surface nature of Pd particles.

XRD, crystallite size, and BET surface area.— Figure 2 shows XRD patterns of the anode catalysts without reduction treatment. Pd was partly formed during decomposition in the presence of ethanol for Pd/SnO_2/C, while only PdO was formed for PdO/C. Formation of any intermetallic compound like Pt_3Sn[24] or alloy was not observed from XRD for the anode catalysts. Figure 3 shows a transmission electron microscope (TEM) image of Pd/SnO_2/C. Light gray particles with diameters of around 4 nm (SnO_2) and dark gray particles (Pd) with diameters of 6–12 nm are uniformly dispersed on C.

Crystallite size of the metal was determined by Scherrer's equation using the width at half maximum of XRD peak for the sample after reduction at 100°C. As shown in Table I, the crystallite size of Pd particles in Pd/C was larger than that of Pt particles in Pt/C. Since the Pd particles grow more easily than Pt particles, the number of Pd active sites for electrochemical oxidation of H_2 was smaller than that of Pt, which is closely related to the cell performances with Pt/C and Pd/C anodes in Fig. 1. The crystallite size of Pd (6.1 nm) in Pd/SnO_2/C is smaller than that (8.2 nm) of Pd/C, while the crystallite size of Pt (2.8 nm) in Pt/SnO_2/C is smaller than that (5.3 nm) of Pt/C. Clearly the SnO_2 addition suppressed the growth of Pd or Pt particles owing to the interaction between precious metals and SnO_2. However, the cell performance was not clearly related to the crystallite size of Pd or Pt particles in Pd/SnO_2/C or Pt/SnO_2/C.

Surface composition.— XPS measurement was carried out to estimate the elemental composition of the surface of each catalyst. The results are shown in Table II. The concentration of Pt or Pd at the surface of Pt/SnO_2/C or Pd/SnO_2/C was lower than nominal one estimated from the source materials for the preparation. It suggests that the SnO_2 patches were covering precious metal particles, and the surface of Pt and Pd particles was partially undetectable by XPS. This was recognized as strong metal and support interaction. Table II also shows the surface composition of the catalysts reduced at 100°C. The concentrations of the precious metals at the surface were not lowered. This means that sintering or migration of the SnO_2 to precious metal did not occur at 100°C. The data also sup-

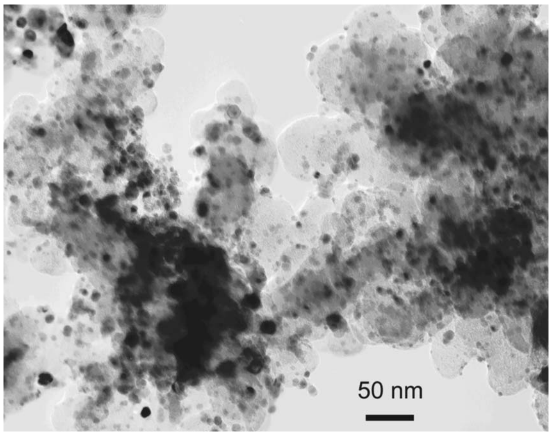

Figure 3. TEM image of Pd/SnO_2/C.

Table I. BET surface areas and crystallite sizes estimated from XRD of the catalysts.

Sample name	Surface area (m^2 g^{-1})	Crystallite size (nm)
C	235	11 (particle size)
SnO_2/C	195	3.1 (SnO_2)
Pd/C	169	8.2 (Pd)
Pt/C	165	5.3 (Pt)
Pd/SnO_2/C	135	6.1 (Pd)
Pt/SnO_2/C	135	2.8 (Pt)

Table II. Surface composition determined by XPS and nominal composition for (SnO_2-modified) Pd and Pt anode catalysts.

	Surface composition (mol %)					Nominal composition (mol %)		
Catalyst	Pt	Pd	PdO	SnO_2	Sn	Pt	Pd	SnO_2
Pt/C	100					100		
Pt/C reduced at 100°C	100							
$Pt/SnO_2/C$	17.8			82.2		43.6		56.4
$Pt/SnO_2/C$ reduced at 100°C	19.4			80.6				
Pd/C		100					100	
Pd/C reduced at 100°C		100						
$Pd/SnO_2/C$		6.5	27.3	66.2			58.6	41.4
$Pd/SnO_2/C$reduced at 100°C		23.2	4.2	67.4	5.2			

port the absence of the intermetallic compounds. If these compounds were formed, the concentration of the precious metal of $Pt/SnO_2/C$ or $Pd/SnO_2/C$ was considerably smaller than that of Pt/C or Pd/C. It is difficult to compare the number of active sites for Pt/C and $Pt/SnO_2/C$, and for Pd/C and $Pd/SnO_2/C$. The surface concentration of Pd in $Pd/SnO_2/C$ was larger than that of Pt in $Pt/SnO_2/C$, though the crystallite size of Pd was larger than that of Pt. The SnO_2 patch should partly cover the surface of Pt particles, and the addition of SnO_2 to Pt/C rather suppressed the electrochemical oxidation activity. On the other hand, Pd particles were stably dispersed on catalyst surface by the addition of SnO_2. From these results, SnO_2 did not cover the surface of Pd particles, and the number of active sites for Pd particles was maintained. Even after the $Pd/SnO_2/C$ anode was reduced in H_2 at 100°C, the 15% of surface Pd was Pd^{2+}, suggesting the strong chemical interaction between Pd and SnO_2. The stably dispersed Pd particles having strong interaction with SnO_2 may contribute to the enhancement of the performance as shown in Fig. 1.

Anodic voltammetry.— The authors reported that the peak potential of CO oxidation over commercial Pt/C (Johnson Matthey) was 0.70 V and CO was oxidized on $Pt/SnO_2/C$ electrode catalyst at 0.74 V.[22] However, it was difficult to observe the CO oxidation on Pd/SnO_2 anode prereduced at 100°C in this experiment. This suggested that Pd/SnO_2 anode catalysts did not adsorb CO easily.

Cell performance in the presence of CO.— Figure 4 shows the effect of SnO_2 addition to Pt/C in the presence of 500 ppm CO. The cell voltages with the Pt/C anode at a current density of 0.2 A/cm^2 drastically dropped from 0.67 to 0.10 V with the addition of 500 ppm CO to H_2. However, the cell voltage with the $Pt/SnO_2/C$ anode dropped from 0.64 to 0.37 V at 0.2 A/cm^2 in CO-contaminated H_2 gas as fuel. Since the cell voltage with the $Pt/SnO_2/C$ anode was higher than Pt/C in the presence of CO, the addition of SnO_2 to Pt/C was effective in developing the CO tolerance for the anode catalyst. There are two mechanisms that can explain CO-tolerant effect. One is the change in *d*-band center of Pt to weaken the interaction between Pt and CO,[16] and another is called a bi-functional mechanism. The reaction between CO adsorbed on Pt and oxygenated species adsorbed on the second metal is promoted via bi-functional mechanism.[7] In addition, it is also reported that the nonelectrochemical water-gas shift reaction on the anode gas diffusion layer lowered CO content in the gas channels of the electrode.[24] In this study, the mechanism of the CO tolerance will be investigated for the $Pt/SnO_2/C$ and $Pd/SnO_2/C$.

Figure 5 shows the effect of SnO_2 addition on the performances of the cell with the Pd anode in 500 ppm CO-contaminated H_2. The $Pd/SnO_2/C$ anode catalyst exhibited higher tolerance to CO poisoning than the Pd/C anode. The cell voltage with the $Pd/SnO_2/C$ anode catalyst at a current density of 0.2 A/cm^2 dropped from 0.59 to 0.41 V in 500 ppm CO-contaminated H_2 gas, and the potential loss resulting from the addition of CO was only 0.18 V. It indicates that the $Pd/SnO_2/C$ anode has high tolerance to CO poisoning. The Pd/C anode itself was higher CO tolerant at low current density around

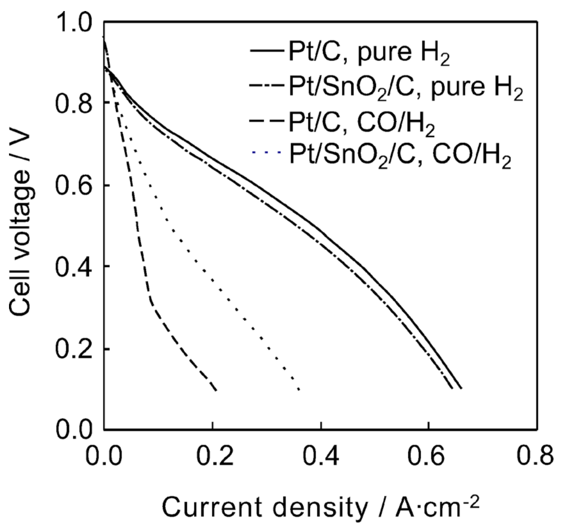

Figure 4. Comparison of the performances of the cells using Pt anodes with/without SnO_2 in the presence of CO. Cathode: Pt/C; anode: Pt/C with/without SnO_2; anode gas: H_2 or 500 ppm CO/H_2; cathode gas: air; cell: 70°C, humidifier: 73°C.

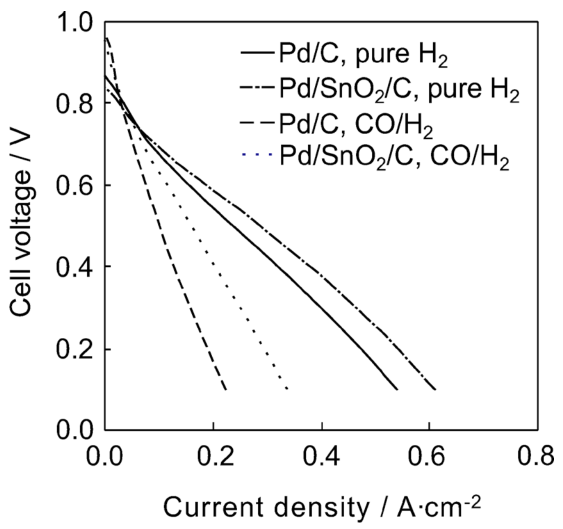

Figure 5. Comparison of the performances of the cells using Pd anodes with/without SnO_2 in the presence of CO. Cathode: Pt/C; anode: Pd/C with/without SnO_2; anode gas: H_2 or 500 ppm CO/H_2; cathode gas: air; cell: 70°C, humidifier: 73°C.

Table III. Electrochemical CO oxidation to CO_2 on anodes in PEFC single cell under power generation condition.

Catalyst	Current density (A cm^{-2})	Cell voltage (V)	CO conv. to CO_2 on anode (%)	CO conv. to CO_2 on anode (%) (at OCV)
Pt/C	0.1	0.2	26.4	(0.09)
$Pt/SnO_2/C$	0.07	0.2	9.2	(0.52)
Pd/C	0.015	0.2	0.8	(0.07)
$Pd/SnO_2/C$	0.02	0.2	1.1	(0.09)
Pt–Ru/C	0.12	0.3	23.2	(0.08)

Cathode: Pt/C; anode: Pt/C or Pd/C with/without SnO_2; anode gas: 5000 ppm CO/H_2; cathode gas: O_2; Cell: 30°C, humidifier: 73°C.

0.1 A/cm^2 than the Pt/C anode. The *I-V* curves of the Pt-type catalysts in Fig. 4 were bent as a result of oxidation of CO, though those of the Pd-type catalysts in Fig. 5 remained almost straight at the same condition. The Pt/C and Pd/C anodes obviously showed different electrochemical activities of CO. The author reported that CO was electrochemically oxidized with voltage drop over 0.7 V on Pt/C anode,[22] which corresponds to the cell voltage less than 0.3 V. As shown in Fig. 4, in the case of the curve of the Pt/C anode during CO poisoning, CO was electrochemically oxidized at the cell voltage less than 0.3 V. Therefore, the voltage drop over 0.07 A/cm^2 was lower than that over 0.3 V under 0.07 A/cm^2 owing to the electrochemical oxidation of CO. On the other hand, for the cells with the $Pd/SnO_2/C$ catalyst, the *I-V* curve was not bent, despite the presence of CO. So, this CO tolerance of $Pd/SnO_2/C$ was not due to electrochemical CO oxidation, and it may be due to the weak adsorption of CO on Pd.

To confirm the effect of electrochemical reaction, electrochemical CO oxidation was evaluated using the same cell in the presence of CO. The adsorbed CO can be also electrochemically oxidized as follows

$$\text{Pt–CO} + H_2O \rightarrow \text{Pt} + CO_2 + 2H^+ + 2e^-$$

CO was electrochemically oxidized above voltage of 0.7 V vs reversible hydrogen electrode (RHE).[22] Therefore, the CO conversion was quantitatively analyzed at the low cell voltage of 0.2 V. The results of electrochemical CO oxidation in the presence of 5000 ppm CO were shown in Table III. Under open-circuit voltage (OCV) condition CO was converted to CO_2 only by shift reaction ($CO + H_2O \rightarrow CO_2 + H_2$), and CO was not electrochemically oxidized to CO_2. The CO conversion at OCV on Pt/C, Pd/C, Pd/SnO_2 and Pt–Ru/C was almost identical and less than 0.1%, while that on $Pt/SnO_2/C$ was 0.5%. This indicated that all shift reaction scarcely contributed to the CO tolerance. Therefore, most of CO_2 in Table II was formed not by shift reaction but by electrochemical CO oxidation. Only for the Pt–Ru/C, the CO conversion was as high as 23.2%. Electrochemical CO oxidation was confirmed at higher cell voltage of 0.3 V, the contribution of electrochemical oxidation to CO resistance was confirmed for Pt–Ru/C catalyst. However, the CO conversion on Pt/C is as high as 26.4%, and the CO conversion rather decreased by the addition of SnO_2 (9.2%). Although contribution of the electrochemical CO oxidation was the largest for Pt/C, Pt did not show the CO tolerance. This means that electrochemical oxidation of CO contributes little to the CO resistance for the Pt/C and $Pt/SnO_2/C$. Electrochemical CO oxidation did not contribute to the CO tolerance for the Pd/C and $Pd/SnO_2/C$ at all. This observation coincided with the fact that CO oxidation was not observed for $Pd/SnO_2/C$ during CO-stripping voltammetry.

Strength of the CO adsorption on precious metal.— The effect of temperature on CO adsorption was measured to estimate the strength of the chemical bond between CO and precious metal. Table IV shows the result of this experiment. The value of this table shows the molar ratio of the CO molecules to precious metal. The number of CO molecules adsorbed on catalysts was divided by the number of precious metal atoms. The Pt/C catalyst adsorbed CO more strongly than the Pd/C catalyst. The results agreed with the data in Fig. 4 that Pt/C was more severely poisoned by CO than $Pt/SnO_2/C$ catalyst. On the other hand, Crabb, Marshall, and Thompsett reported that the addition of tin to Pt/C suppresses chemisorption of both hydrogen and CO.[25] In this case, degradation of the cell voltage was observed when Pt/Sn/C was used as anode catalyst. In the present investigation, the addition of SnO_2 to Pt/C and Pd/C catalysts did not cause degradation of the cell voltage.

Figure 6 shows the influence of temperature upon the amount of CO adsorbed on each precious metal, based on Table IV. The amount of CO adsorbed on each precious metal at 25°C was defined as 100% for the reference. Clearly Pd/C desorbed CO more easily than Pt/C. When the sample was heated to 300°C in flowing He, adsorbed water on the catalyst was expected to be removed. Then, the bi-functional mechanism[7] did not take place under this examination condition. The decrease in CO adsorption was due to weakened CO adsorption. Figure 6 indicates that Pt/C strongly adsorbed CO, since 40% of CO adsorbed on Pt/C at 25°C remained at 300°C. On the other hand, the relative amount of CO adsorbed on

Table IV. Molar ratio of adsorbed CO/precious metal.

	Molar ratio of adsorbed CO to precious metal (%)			
Temp. (°C)	Pt/C	$Pt/SnO_2/C$	Pd/C	$Pd/SnO_2/C$
25	27.0	13.3	7.0	5.4
60	25.5	12.5	6.2	4.8
90	24.4	11.7	5.5	4.2
120	23.0	10.6	4.8	3.6
150	21.4	9.6	4.1	2.7
180	19.7	8.5	3.3	2.0
210	18.8	6.9	2.5	1.4
240	16.8	5.1	1.8	0.7
270	14.4	3.5	1.2	0.5
300	10.4	1.8	1.1	0.3

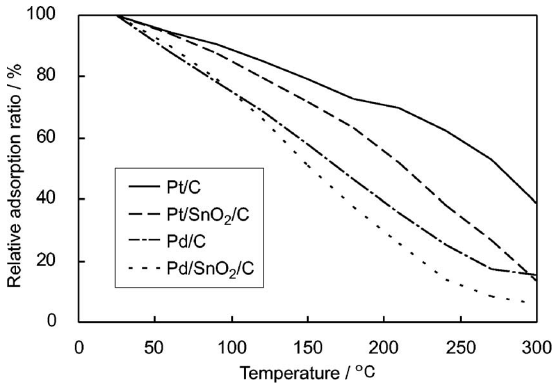

Figure 6. Temperature dependence of CO adsorbed on several Pt or Pd catalysts.

$Pt/SnO_2/C$ was 15% at 300°C, so that the chemical bond for the adsorption should be weak. In the same way, the CO adsorption on $Pd/SnO_2/C$ was weaker than that on Pd/C. Especially, the relative amount of CO adsorbed on the $Pd/SnO_2/C$ at 150°C was half of that at 25°C. So, the strength of CO adsorption on Pt or Pd was weakened when SnO_2 nanoparticles were added to the catalysts. This behavior of the CO adsorption on these $Pt/SnO_2/C$ and $Pd/SnO_2/C$ catalysts agreed with the *I-V* curves in the presence of CO. Therefore, the CO tolerance and the bonding strength between CO and precious metal were closely related. Weakly adsorbed CO on the precious metals may contribute to the CO tolerance. Consequently, the high CO tolerance of these catalysts is due to the strong interactions between precious metal and SnO_2 nanoparticles. The results suggest that weakening of CO adsorption on precious metal was important for improvement of CO tolerance.

Effect of reduction temperature on the strength of CO adsorption on precious metal.— The CO adsorption on the precious metals was measured to estimate the effect of reduction temperature on the bonding strength between CO and precious metal. The importance of the intimate mixing of Pt and the second elements was claimed by Götz and Wendt.[8] The reduction temperature of the catalyst would affect CO tolerance. Table V shows the result of the effect of reduction temperature. The Pd-containing catalysts reduced at 200°C adsorbed smaller amount of CO than the Pt-containing catalyst. The amount of CO adsorbed on the Pd-containing catalyst was about half of that on the Pt-containing catalysts. The addition of SnO_2 nanoparticles clearly reduced the amount of CO adsorbed. The reduction temperature did not strongly affect the amounts of CO adsorbed on Pt/C and Pd/C, while those on $Pt/SnO_2/C$ and $Pd/SnO_2/C$ were strongly affected. This fact indicates the interactions between Pt and SnO_2 and between Pd and SnO_2 and each other despite low reduction temperature or under moderate reduction atmosphere like PEFC-operating conditions. Therefore, the reduction condition that can be encountered in the anode atmosphere of PEFC contributed to the high CO tolerance of the SnO_2-containing catalysts.

Table V. Molar ratio of adsorbed CO/precious metal.

Catalyst	Reduction temperature (°C)	Molar ratio of adsorbed CO/Pt, Pd (%)
Pt/C	100	22.5
	200	20.1
$Pt/SnO_2/C$	100	19.3
	200	10.0
Pd/C	100	9.5
	200	7.0
$Pd/SnO_2/C$	100	5.3
	200	0.5

Conclusion

The CO tolerance of the PEFC anode catalyst was improved by addition of SnO_2 nanoparticles. The SnO_2 addition to the anode somewhat decreases the electrochemical activity in pure H_2, but clearly increases the CO tolerance of the anode catalysts. It was revealed by CO pulse titration that the SnO_2-containing catalysts adsorbed CO more weakly than the other catalysts without SnO_2 nanoparticles. This phenomenon was derived from the interaction between Pt or Pd atoms and SnO_2 nanoparticles, since these catalysts mixed with carbon did not exhibit intermetallic compounds. The $Pd/SnO_2/C$ anode exhibited the highest tolerance to CO poisoning among the catalysts.

Acknowledgment

This study was supported by the Industrial Technology Research Grant Program in 02B61003c from the New Energy and Industrial Technology Development Organization (NEDO) of Japan.

Hokkaido University assisted in meeting the publication costs of this article.

References

1. M. Yoshimura, Y. Hori, Y. Tsuji, A. Yoshida, T. Yonamine, and M. Uchida, Jpn. Kokai Tokkyo Koho, JP A 2005–216834 A (2005).
2. R. G. Herman, K. Klier, G. W. Simmons, B. P. Finn, J. B. Bulko, and T. P. Kobylinski, *J. Catal.*, **56**, 407 (1979).
3. M. M. Gadgil, R. Sasikala, and S. K. Kulshreshtha, *J. Mol. Catal.*, **87**, 297 (1994).
4. M. Haruta, S. Tsubota, T. Kobayashi, H. Kageyama, K. J. Genet, and B. Delmon, *J. Catal.*, **144**, 175 (1993).
5. M. Echigo, N. Shinke, S. Takami, S. Higashiguchi, K. Hirai, and T. Tabata, *Catal. Today*, **84**, 209 (2003).
6. M. Okumura, N. Masuyama, E. Konishi, S. Ichikawa, and T. Akita, *J. Catal.*, **208**, 485 (2002).
7. M. Watanabe and S. Motoo, *J. Electroanal. Chem. Interfacial Electrochem.*, **60**, 267 (1975).
8. S. Mukerjee, R. C. Urian, S. J. Lee, E. A. Ticianelli, and J. McBreen, *J. Electrochem. Soc.*, **151**, A1094 (2004).
9. M. Götz and H. Wendt, *Electrochim. Acta*, **43**, 3637 (1998).
10. T. Ioroi, K. Yasuda, Z. Siroma, N. Fujiwara, and Y. Miyazaki, *J. Electrochem. Soc.*, **150**, A1225 (2003).
11. A. Ueda, Y. Yamada, T. Ioroi, N. Fujiwara, K. Yasuda, Y. Miyazaki, and T. Kobayashi, *Catal. Today*, **84**, 223 (2003).
12. T. Matsui, K. Fujiwara, T. Okanishi, R. Kikuchi, T. Takeguchi, and K. Eguchi, *J. Power Sources*, **155**, 152 (2006).
13. E. Antolini, *Mater. Chem. Phys.*, **78**, 563 (2003).
14. E. Christoffersen, P. Liu, A. Ruban, H. L. Skriver, and J. K. Norskov, *J. Catal.*, **199**, 123 (2001).
15. A. S. Arico, Z. Poltarzewski, H. Kim, A. Morana, N. Giordano, and V. Antonucci, *J. Power Sources*, **55**, 159 (1995).
16. W. Zhou, Z. Zhou, S. Song, W. Li, G. Sun, P. Tsialaras, and Q. Xin, *Appl. Catal., B*, **46**, 273 (2003).
17. L. Jiang, G. Sun, Z. Zhou, S. Sun, Q. Wang, S. Yan, H. Li, J. Tian, J. Guo, B. Zhou, and Q. Xin, *J. Phys. Chem. B*, **109**, 8774 (2005).
18. A. L. Santos, D. Profeti, and P. Olivi, *Electrochim. Acta*, **50**, 2615 (2005).
19. M. B. de Oliveira, L. P. R. Profeti, and P. Olivi, *Electrochem. Commun.*, **7**, 703 (2005).
20. M. Nakada, A. Ishihara, S. Mitsushima, N. Kamiya, and K. Ota, *Electrochem. Solid-State Lett.*, **10**, F1 (2007).
21. T. Okanishi, T. Matsui, T. Takeguchi, R. Kikuchi, and K. Eguchi, *Appl. Catal., A*, **298**, 181 (2006).
22. T. Matsui, K. Fujiwara, T. Okanishi, R. Kikuchi, T. Takeguchi, and K. Eguchi, *J. Power Sources*, **155**, 152 (2006).
23. J. Zhang and Lian Gao, *Chem. Lett.*, **32**, 458 (2003).
24. E. I. Santiago, M. S. Batista, E. M. Assaf, and E. A. Ticianelli, *J. Electrochem. Soc.*, **151**, A944 (2004).
25. E. M. Crabb, R. Marshall, and D. Thompsett, *J. Electrochem. Soc.*, **147**, 4440 (2000).